

The Effect of Trace Amount of H₂S on CO₂ Corrosion Investigated by Using the EIS technique

Kun-Lin John Lee and Srdjan Nestic

**Institute for Corrosion and Multiphase Flow Technology
Ohio University, Athens, OH 45701, USA**

Abstract

A project has been initiated with the aim of extending the model to cover the effect of H₂S on CO₂ corrosion. This report covers one of the main building blocks necessary to complete the mechanistic CO₂/H₂S corrosion model, namely, electrochemistry of API 5L X65 carbon steel CO₂ corrosion in the presence of small amounts of H₂S (≤ 340 ppm). The corrosion process monitored by Linear Polarization Resistance (LPR) and Electrochemical Impedance Spectroscopy (EIS) showed a significant decrease in corrosion rate in the presence of H₂S due to the metal surface coverage by a sulfide film. This sulfide film was identified as mackinawite by X-ray photoelectron spectroscopy (XPS). Since the experimental results suggested that the mechanism is a retardation of the charge transfer process, the surface coverage was calculated from the corrosion rate. The Langmuir-type adsorption isotherm was successful in modeling the surface coverage by mackinawite in the presence of trace amounts of H₂S.

Introduction

The advantage of EIS technique over other electrochemical experimental techniques in studying corrosion has been discussed in the previous work.¹ This report extends the EIS investigation of the electrochemical reaction in saturated CO₂ solution with slightly higher H₂S concentrations (0~340ppm) in a low temperature, low pressure and low pH condition over longer immersion time (4~72 hours).

It has been speculated previously that the protective thin sulfide film might have formed at the electrode surface via solid state formation,² resulting in a lower corrosion rate in the presence of trace amount of H₂S. Numerous reports have hinted that this thin sulfide film may possibly be mackinawite (FeS_{1-x}).²⁻¹³ Hence, providing direct evidence that confirms the existence of thin mackinawite film on the electrode was one of the main goals of this study.

However, this very thin film was not visible to the naked eye, as the electrode surface remained shiny throughout the experiment due to the low corrosion rate. Scanning

Electron Microscopy (SEM), which examines the electrode surface, was incapable of observing such a thin layer of film. Although X-ray Diffraction analysis (XRD) is a popular technique that enables one to distinguish different types of thin iron sulfide on a flat surface, it is not suitable for a round surface on the cylindrical electrode. On the other hand, even though Electron Dispersion Spectroscopy (EDS) technique had detected sulfide elements on the electrode surface, it was not able to confirm the exact iron sulfide compound.¹⁴ In order to clarify the exact chemical composition of this thin protective sulfide film, the electrode surface was examined using X-ray photoelectron spectroscopy (XPS).

Surface analysis by XPS is accomplished by irradiating the target surface with soft x-rays and analyzing the energy of the detected electrons. The x-rays interact with atoms in the surface region, causing electrons to be emitted by the photoelectric effect. The emitted electrons have measured kinetic energy given by:

$$KE = h\nu - BE - \phi_s \quad (1)$$

where $h\nu$ (eV) is the energy of the photon (x-ray), BE (eV) is the binding energy of the atomic orbital from which the electron originates, and ϕ_s (eV) is the spectrometer work function.

The binding energy is the energy difference between the initial and final states after the photoelectron has left the atom. Since each element has a unique set of binding energies, XPS can be used to identify and determine the concentration of the elements in the surface. Slight variation in the elemental binding energies (the chemical shifts) arises from the chemical potential of compounds. These chemical shifts can be used to identify the chemical states of the materials being analyzed and it is very effective for determining various types of iron sulfides.

Experiment

Experiments were conducted in a glass cell on carbon steel X65 at these conditions: $T = 20^\circ\text{C}$, $\text{pH} = 5$, $P = 1$ bar, $\omega = 1000$ rpm, gaseous H_2S concentration in $\text{CO}_2 = 0, 3, 15, 40, 160$ and 340 ppm. In these experiments the corrosion process was monitored with different electrochemical measuring techniques: Electrochemical Impedance Spectroscopy (EIS) and Linear Polarization Resistance (LPR). Experiments for each H_2S concentration were conducted at least twice to make sure that the results were reproducible and reliable.

Equipment

Experiments were conducted at atmospheric pressure in a glass cell at room temperature. Gas (with varied concentration of H_2S in CO_2) was continuously bubbled through the cell. A three-electrode set-up (Figure 1) was used in all electrochemical experiments. A rotating cylinder electrode with a speed control unit was used as the working electrode. A concentric graphite ring was used as a counter electrode. A saturated Ag/AgCl reference

electrode was used and was externally connected to the cell via a Luggin capillary and a porous wooden plug. The pH was followed with an electrode directly immersed into the electrolyte. Outlet H₂S and CO₂ gases were scrubbed by gas absorbent. Electrochemical measurements were made with a potentiostat connected to a PC.

Material

A typical construction API 5L X65 carbon steel was tested. The chemical composition of the steel is given in Table 1. The working electrode was machined from the parent material into a cylinder 12 mm in diameter and 14.3 mm long. The exposed area of the specimen was 5.4 cm².

Experimental Procedure

The glass cell was filled with 2 liters of electrolyte: de-ionized distilled water + 3 wt% NaCl. Initially CO₂/H₂S gas, was bubbled through the electrolyte, (at least one hour prior to experiments) in order to saturate and deaerate the solution. Monitoring of pH was used to determine whether the solution is in equilibrium. x %/mM solution of NaHCO₃ was deaerated before it was added to adjust the solution to pH 5. During the experiment, constant concentration of H₂S in CO₂ gas was continuously bubbled through the electrolyte in order to maintain consistent water chemistry. The gaseous H₂S concentration was maintained precisely by fixing the flow rate ratio of CO₂ to H₂S with a gas rotameter. The gaseous concentration of H₂S was verified by colorimetric tube before the experiment was conducted. The steel working electrode surface was then polished with 220 and 600 grit silicon carbide papers, washed with alcohol, mounted on the specimen holders, and immersed into the electrolyte. The free corrosion potential was monitored immediately after immersion.

After 20 minutes of immersion at the free corrosion potential, EIS measurements were conducted by applying an oscillating potential ± 5 mV around the free corrosion potential to the working electrode using the frequency range 0.001 Hz-5000 Hz. The Linear Polarization Resistance (LPR) technique was used to measure the polarization resistance R_p and thus the corrosion rate could be determined. Depending on the experimental conditions, the author did not terminate the experiment unless the process reached steady state. The experimental conditions are listed in Table 2.

Results and discussion

Before any experiments were conducted using the EIS technique in slightly sour environments, a number of baseline experimental results needed to be established in the absence of H₂S to serve as reference points in order to better understand the role of H₂S on the corrosion of carbon steel.

Figure 2 demonstrates the effect of 3 ppm H₂S concentration on the characteristics of the impedance plots at the corrosion potential. For carbon steel X65 in the pH 5 H₂S-free saturated CO₂ solution at corrosion potential, the impedance diagram exhibits a depressed semicircle at high frequencies indicating a double-layer capacitance, as well as an inductive loop at lowest frequencies. A depressed semicircle is not uncommon for iron dissolution in acidic media and it was suggested in the literature that the heterogeneous surface roughness and the nonuniform distribution of current density on the surface may be related to it.^{15,16} The Nyquist impedance diagram showed no mass transfer controlled impedance under these conditions; however, it was not a pure charge transfer controlled process either because the inductive loop at low frequencies indicated that the iron dissolution mechanism might occur in two steps involving an adsorbed intermediate. According to Keddam et al.,^{17,18} the inductive loop at the low frequency was related to the relaxation time of the intermediate adsorbed species, (FeHCO₃)⁺_{ad}. Moreover, the characteristics of the impedance diagram did not change after 4 hours of immersion.

With the addition of 3 ppm gaseous H₂S, the steady-state impedance diagram at corrosion potential demonstrated a larger diameter of depressed semicircle with similar characteristics. Moreover, the polarization resistance (R_p) values that intercepted the real axis of the Nyquist plot are three times larger than that of the H₂S free solution, matching a lower corrosion rate of 0.28 mm/year measured by LPR (shown in Figure 4). These results suggest that the mechanism is still charge-transfer controlled in the presence of 3ppm gaseous H₂S, but the sulfide film detected on the electrode surface (using EDS)¹⁴ had inhibited the corrosion rate by a coverage effect. It was unnecessary to use equivalent circuit to analyze the impedance data because all the data exhibited a charge transfer controlled characteristics.

In order to investigate the effect of very small H₂S concentrations, other sets of experiments were conducted by saturating the solution with 15 ppm, 40 ppm, 160 ppm and 340 ppm of gaseous H₂S in CO₂, while keeping all other conditions the same. The steady-state Nyquist plot shown in Figure 3 demonstrates that the diameter of depressed semicircle increases with increasing H₂S concentration, while maintaining similar characteristics and exhibits only charge-transfer controlled behavior. On the other hand, the increase in polarization resistance R_p from EIS measurements also indicated the decrease in corrosion rate with increasing H₂S concentration. The R_p from both EIS and LPR measurements were converted into corrosion rate and a good agreement was reached between the two techniques (illustrated in Figure 4). From the above evidence, it can be concluded that a very thin iron sulfide film did not act as a diffusion barrier, but rather had retarded the corrosion by a "coverage effect" under these experimental conditions. Although the surface coverage effect strongly depends on H₂S concentration, the inhibition of corrosion rate reaches plateau at 0.06 mm/year and ceases to decrease significantly beyond 160 ppm of H₂S concentration.

One can observe how the depressed semicircle increases in diameter over time in Figure 5, which demonstrates the transient characteristics of the Nyquist impedance diagram in the presence of 340 ppm gaseous H₂S. The initial EIS measurement (taken after 20 minutes of immersion) suggests that a protective thin sulfide film had formed via solid

state formation² at the electrode surface almost immediately after immersion. The low-frequency data (the initial EIS measurement) that drift below the x-axis are not an instrumental error, but indicate the transient increase of polarization resistance (R_p) during the long EIS measurement, hence illustrating the increase of surface coverage over time. By the end of first EIS measurement, the electrode had been immersed in the solution for 4 hours and the lowest frequency ($f=0.001$) data point indicated that R_p reached 394 ohm (denoted by the larger marker), matching a low corrosion rate of 0.08 mm/year (measured by LPR). Comparing to the corrosion rate of H₂S-free solution (0.84 mm/year), this result suggests that mackinawite film had achieved a ten-fold inhibition of corrosion rate within 4 hours of immersion under the experimental condition. The characteristics of the impedance diagram stopped changing after 36 hours of immersion indicating that the sulfide film had reached an equilibrium and the corrosion rate remained constant throughout the rest of the experiment.

In a parallel study, a large number of carefully controlled corrosion experiments has been conducted in flow loop under different temperatures (60 °C and 80°C), partial pressures of CO₂ (7.7 bar) and velocities (stagnant to 3 m/s) in both single and multiphase flow.¹⁹ The results obtained from the flow loop experiments (under high temperature and high pressure) have very similar trends compared to that of glass cell experiment (low temperature and low pressure). All the experimental data clearly indicate that the presence of even very small amounts of H₂S (10 ppm in the gas phase) leads to rapid and drastic reduction in the corrosion rate. However, this trend does not extend or even slightly reverses at higher H₂S concentration. The effect seems to be universal and depend only on the H₂S concentration because all the data obtained at very different conditions follow the same trend, as shown in Figure 6. The corrosion rate in Figure 6 was normalized with the "pure" CO₂ corrosion rate that was obtained in the absence of H₂S.

Surface Analysis

X-ray photoelectron spectra were obtained with a Kratos Ultra Axis electron energy analyzer using an Al K α non-monochromatic source (1486.6 eV). The base pressure in the analytical chamber was of the order of 10⁻⁹ mbar. The energy scale was calibrated using the Ag(3d_{5/2})(368.2 eV) lines. Survey and narrow XPS spectra were obtained with an analyzer pass energy of 80 and 20 eV, respectively. Raw spectra were smoothed before being fitted using a Shirley base line and a Gaussian-Lorentzian shape peak. The aliphatic adventitious hydrocarbon C(1s) peak at 284.6 eV was adopted as a check for surface charging.

The XPS survey scan of the sample (retrieved after 72 hours of immersion in a saturated CO₂ solution with gaseous concentration of 340 ppm H₂S and 3% NaCl) indicated the presence of O, C, Na, Cl, Fe and S at the sample surface (shown in Figure 7). Even by taking precautions during the preparation of the sample for analysis, it was not possible to completely eliminate oxygen that adsorbed at the surface. Otherwise, carbon was an ubiquitous contaminant.

The narrow region spectra for Fe(2p_{3/2}) and S(2p) are shown in Figure 8 and Figure 9, respectively. No charge correction was necessary. The Fe(2p_{3/2}) spectrum consists of two major contributions occurring at 710.4eV and 712.1eV, the second peak corresponds to the chemical shift in the photoelectron binding energy of mackinawite from elemental iron Fe.^{20,21} On the other hand, the S(2p) spectrum presents a major contribution which has peak occurring at 162.3 eV, which also matches the shift in photoelectron binding energy of mackinawite from elemental sulfur S.^{20,21} Furthermore, the semi-quantitative surface composition ($\pm 10\%$) was calculated from the peak areas and theoretical cross-sections,²² giving Fe:S atomic mass concentration ratio of 1 to 0.847, which matches the chemical composition of mackinawite (FeS_{1-x})^{3,4,12,23} and supports the analysis of the spectra. Hence, it can be concluded that mackinawite film had inhibited the corrosion by a coverage effect under these experimental conditions.

Mathematical Model

The above mentioned experimental results suggest that iron sulfide films such as mackinawite can form on the surface of the steel via solid state reaction regardless of whether supersaturation is exceeded or not, which agreed with previous research done by Shoosmith et al.² These iron sulfide films appear to have two effects: they inhibit the corrosion process by surface coverage of mackinawite (dominant at very low H₂S concentrations) and may even have a catalytic effect at higher H₂S concentrations, e.g. by providing an increased area for the cathodic reaction. From EIS measurements, it was observed that the mechanism is not of mass-transfer control, but rather charge-transfer controlled. In order to account for the inhibition of a charge transfer reaction at the electrode surface, an equation including a simple Langmuir type adsorption isotherm and a first order catalytic effect was successfully used to model the decrease of the corrosion rate:

$$1 - \theta_{H_2S} = \frac{1}{1 + K_{a/d} c_{H_2S}} + k_c c_{H_2S} \quad (2)$$

where $K_{a/d}$ = the adsorption/desorption constant for sulfide species (units ...)
 k_c = the catalytic rate constant.

This model was verified by comparing the predictions with experimental results as illustrated in Figure 10

Conclusions

- XPS analysis confirmed the presence of mackinawite (FeS_{1-x}) on the electrode surface under these experimental conditions.
- Mackinawite was formed immediately on the electrode via solid state formation in CO₂ solution with trace amount of H₂S.

- Under these experimental conditions, the mackinawite film did not act as a diffusion barrier, but rather had inhibited the corrosion by a coverage effect.
- The Frumkin-type adsorption isotherm was successful in modeling the surface coverage by mackinawite in the presence of trace amounts of H₂S.

Acknowledgements

During this work, Kun-Lin John Lee has been supported by a Stoker Fund from the Chemical Engineering Department, Ohio University. The authors would like to acknowledge the contribution of a consortium of companies whose continuous financial support and technical guidance led to the development of the present model. They are: BP, Champion Technologies, Chevron Texaco, ConocoPhillips, ENI, ExxonMobil, MI Technologies, Ondeo Nalco, Saudi Aramco, Shell, Total and TR Oil .

The authors wish to thank Lisa Hommel, from Surface Analysis Facility of Ohio State University, for her technical support in surface analysis using XPS. The authors would also like to thank Daniel Mosser, for his effort in drawing the 3-D schematic of the experimental test cell (shown in Figure 1).

References

1. K-L J. Lee and S. Netic, "EIS Investigation in the Electrochemistry of CO₂/H₂S corrosion", Corrosion/04, paper no. 728 (New Orleans: NACE International, 2004).
2. D.W. Shoesmith, P. Taylor, M.G. Bailey, D.G. Owen, J. Electrochem. Soc. 127 (1980) p.1007.
3. D.T. Rickard, "The Chemistry of iron sulfide formation at low temperatures". Stockholm Contrib. Geol. 26 (1969), p. 67-95.
4. R.E. Sweeney, I.R. Kaplan, "Pyrite framboid formation: laboratory synthesis and marine sediments". Geology. Vol. 68, (1973) p. 618-634.
5. E.C. Greco, W.B. Wright, Corrosion, v.18, p. 119t-124t (1962)
6. S.P. Ewing, "Electrochemical studies of the hydrogen sulfide corrosion mechanism", Corrosion 11 (1955): p.51
7. T.A. Ramanarayanan and S.N. Smith, "Corrosion of iron in gaseous environments and in gas-saturated aqueous environments", corrosion v. 46 no.1 p.66 (1990).
8. S.N. Smith, "A proposed mechanism for corrosion in slightly sour oil and gas production", 12th international corrosion congress, Houston, TX, September 1993.
9. H.Vedage, T.A. Ramanarayanan, J.D. Mumford and S.N. Smith, "Electrochemical growth of iron sulfide films in H₂S-saturated chloride media", corrosion, v. 49, no.2, p.114-121 (1993).
10. S.N. Smith and E.J. Wright, "Prediction of minimum H₂S levels required for slightly sour corrosion", Paper NO.11, CORROSION/94
11. R.A. Berner, "Iron sulfides formed from aqueous solutions at low temperatures and pressures". J. Geol. Vol. 72, (1964) p. 293-306.
12. R.A. Berner, "Thermodynamic stability of sedimentary iron sulfides". Am. J. Sci. Vol. 265, (1967) p. 773-785.
13. J.B. Sardisco, W.B. Wright, E.C. Greco, Corrosion 19 (1963) p.354
14. B. Brown, Srdjan Netic and Shilpha Reddy Parakala, "CO₂ Corrosion in the presence of Trace Amounts of H₂S", paper 736, (New Orleans, LA: NACE International, 2004)

15. E. McCafferty, *Corros. Sci.* 39 (1997) 243.
16. D.D. MacDonald, M.C.H. Mckubre, J.O.M. Bockris, B.E. Conway, R.E. White (Eds.), *Modern Aspects of Electrochemistry*, vol. 14, Plenum Press, New York, 1982, p.61
17. M. Keddam, O.R. Mattos, H. Takenouti, *J. Electrochem. Soc.* 128 (1981) p.257.
18. M. Keddam, O.R. Mattos, H. Takenouti, *J. Electrochem. Soc.* 128 (1981) p.266.
19. B. Brown, K-L J. Lee, Apr. 2002, Board Meeting report, Ohio University.
20. H. Binder, *Z. Naturforsch* (1973). B28, p.256
21. Y. Limouzin-Maire, *Y. Bull. Soc. Chim. Fr.* (1981) I. p.340
22. J.H. Scofield, *Electron. Spectrosc. Related Phenom.* 8 (1976), p.129-137.
23. A.R. Lennie and D.J. Vaughan, "spectroscopic studies of iron sulfide formation and phase relations at low temperatures", *Mineral Spectroscopy: A tribute to R.G. Burns.* 5 (1996), p.117-131.
24. V.J. Drazic and D.M. Drazic, "Influence of the metal dissolution rate on the anion and Inhibitor adsorption", *Proc. 7th European Symposium on Corrosion Inhibitors (7SEIC): Ann. Univ. Ferrara, N.S., Sez. V, Suppl. N. 9, 1990 (Ferrara, 1990), p.99*

Table 1. Chemical composition of the API 5L X65 carbon steel used for the working electrode (mass%)

C	Mn	Si	Nb	V	Fe	P	S	Cr	Cu	Ni	Mo	Al
0.150	1.34	0.24	0.03	0.055	Balanced	0.011	0.004	0.011	0.01	0.02	0.103	0.032

Table 2. Experimental conditions

Test solution	Water + 3 mass% NaCl
Test material	API 5L X65 Carbon steel
Temperature	20°C
Pressure	1 bar
pH	5
Fe ⁺⁺	<1 ppm
Rotational speed	1000 rpm
Gaseous H ₂ S concentration in CO ₂	0, 3, 15, 40, 160, 340 ppm
Scan rate	0.125 mV/s
Polarization scan	From -5 to +5 mV vs. E _{oc}
Potentiostatic EIS	
DC current	0 mV vs. E _{corr}
AC potential	±5 mV
Frequency range	0.001 – 5000 Hz
Test duration	4 – 72 hours

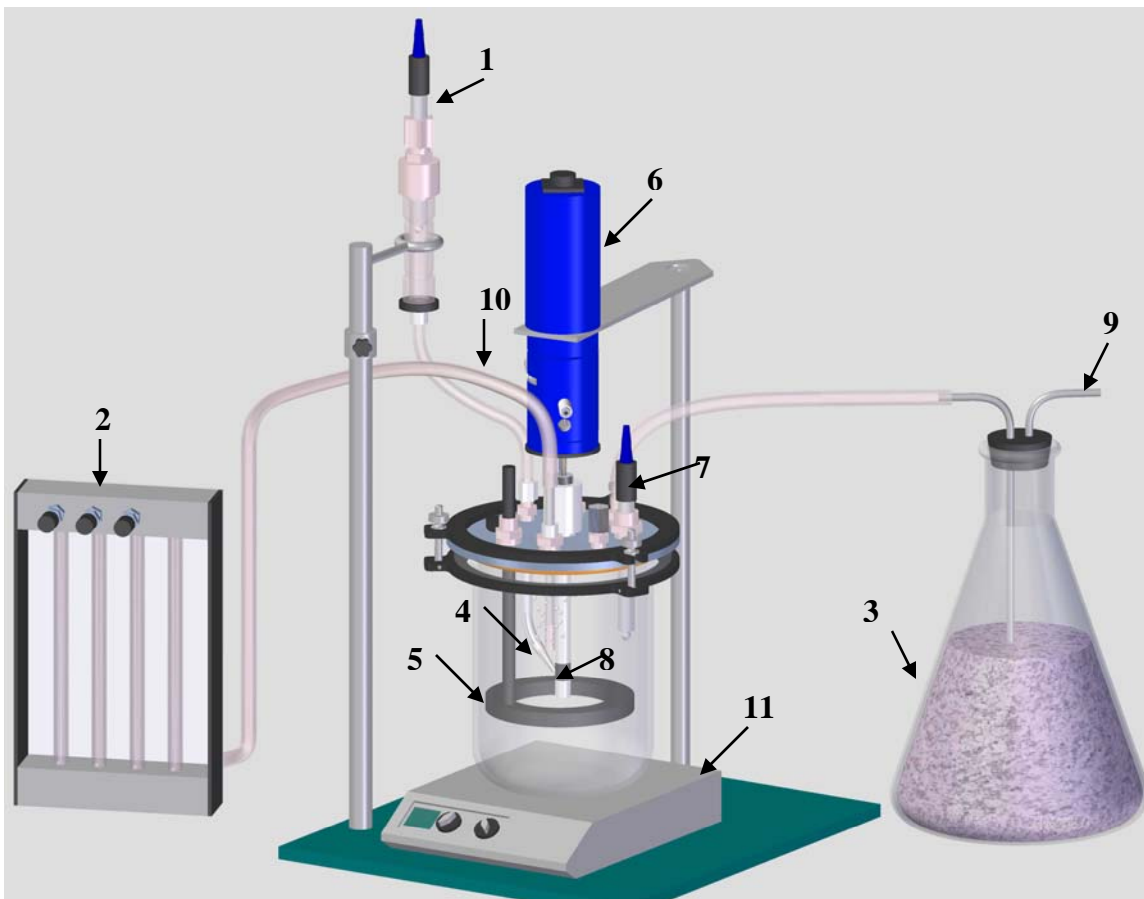


Figure 1. Schematic of the experimental test cell: 1-Ag/AgCl reference electrode, 2-gas rotameter, 3-H₂S scrubber (gas absorbent) , 4-Luggin capillary, 5-graphite counter electrode, 6-rotator, 7-pH electrode, 8-working electrode, 9-gas out, 10-gas in, 11- temperature control unit/stirrer.

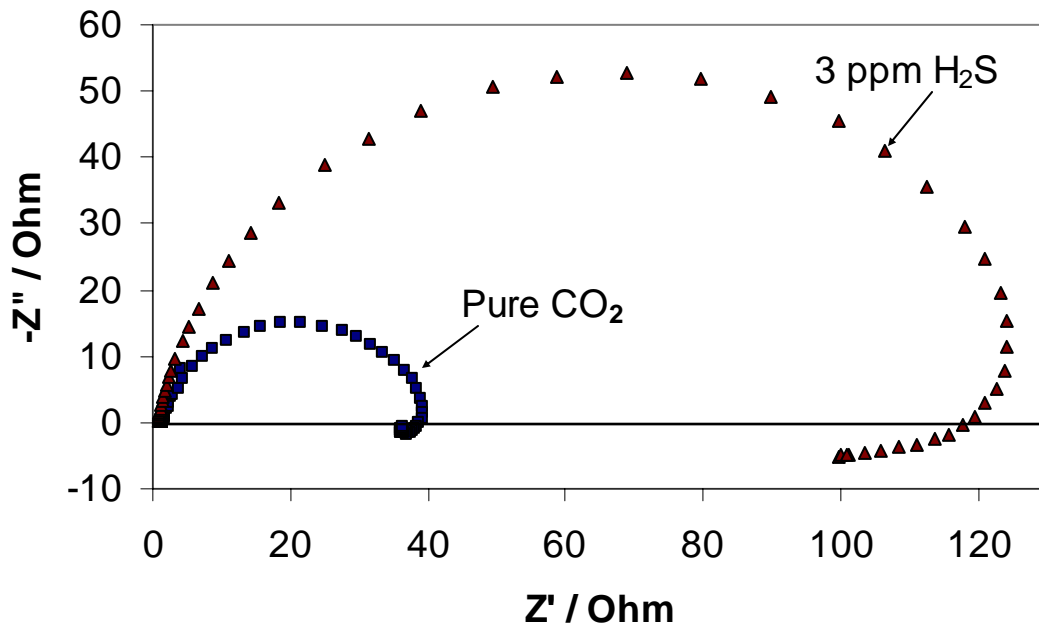


Figure 2. Effect of 3 ppm gaseous H₂S on the Nyquist impedance diagram for carbon steel X65 in pH 5 saturated CO₂ solution of water + 3% NaCl, p = 1 bar, t = 20°C, ω = 1000 rpm at corrosion potential (vs. Ag/AgCl).

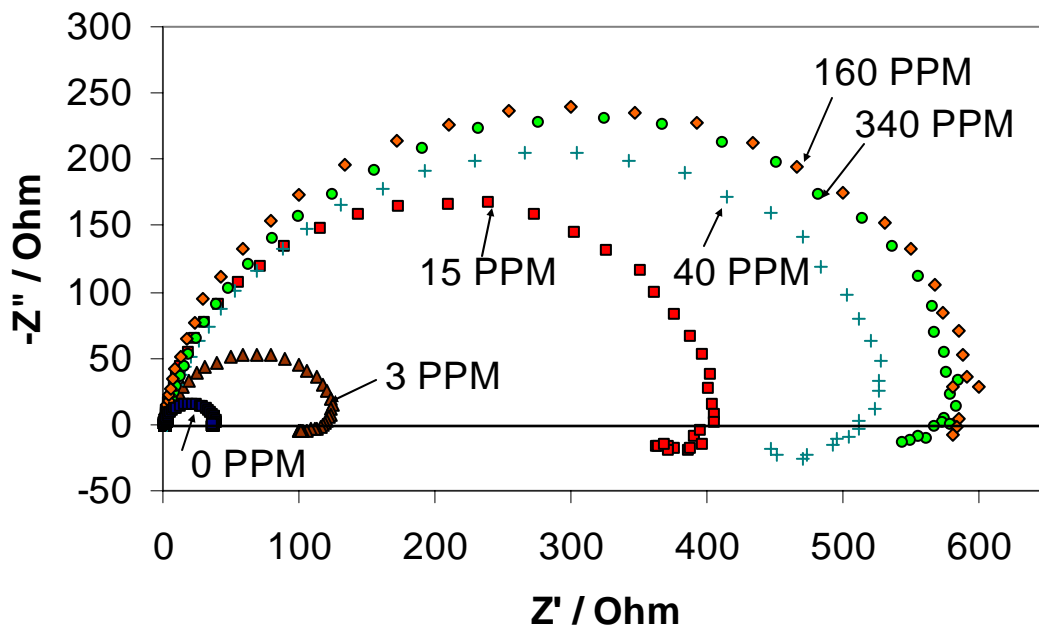


Figure 3. Effect of gaseous H₂S concentration on the steady-state Nyquist impedance diagram for carbon steel X65 in pH 5 saturated CO₂ solution of water + 3% NaCl, p = 1 bar, t = 20°C, ω = 1000 rpm at corrosion potential.

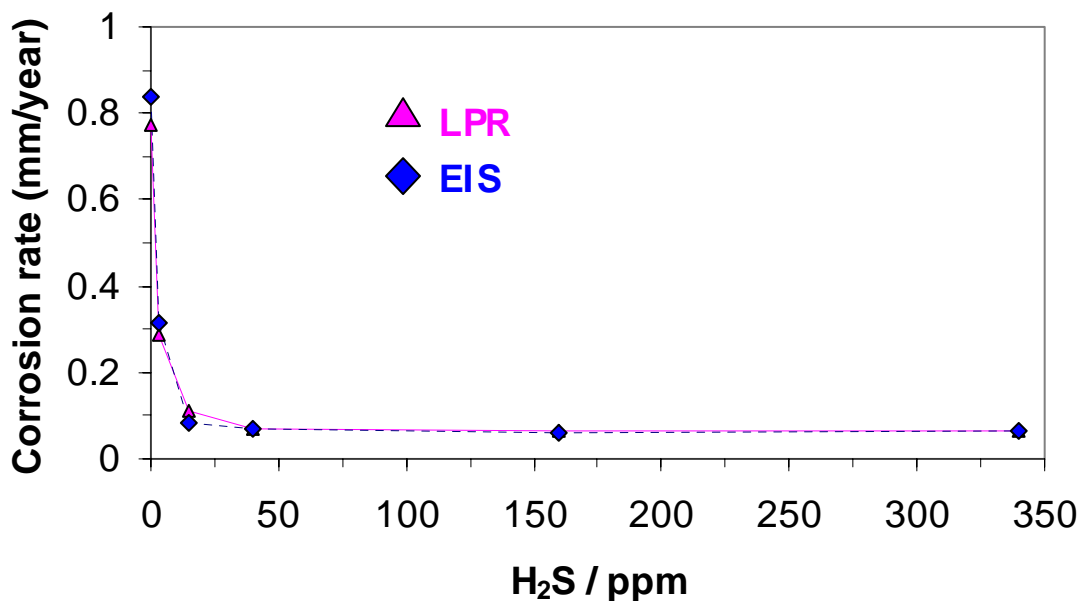


Figure 4. Effect of H₂S gaseous concentration on the final stabilized corrosion rate (measured by LPR and EIS) of carbon steel X65 in pH 5 saturated CO₂ solution, water + 3% NaCl, p = 1 bar, t = 20°C, ω = 1000 rpm. Experiments were repeated for each H₂S concentration.

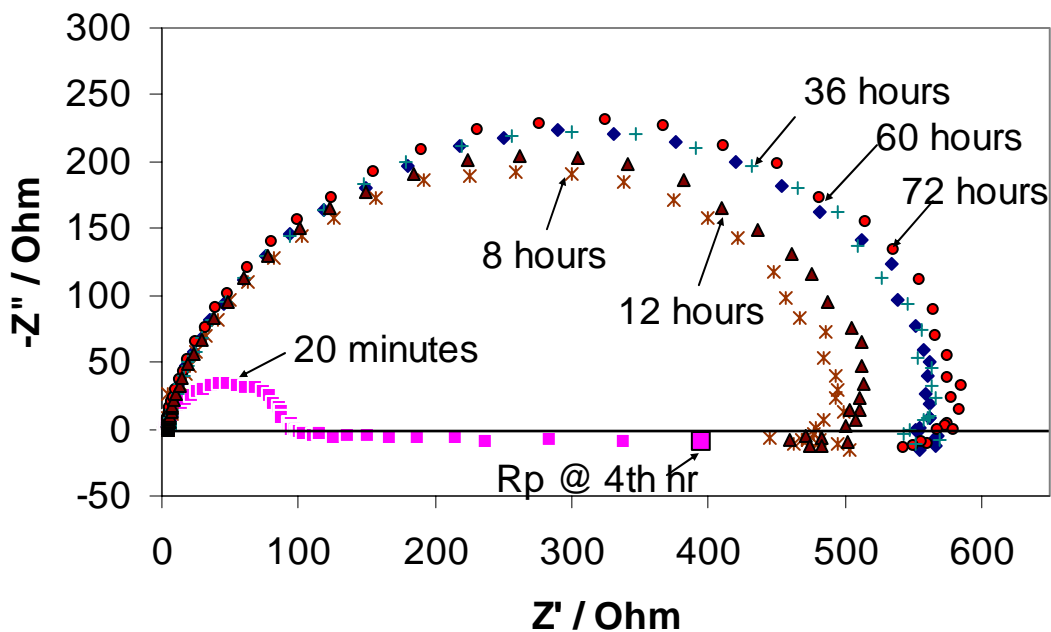


Figure 5. Effect of immersion time on Nyquist impedance diagram of carbon steel X65 in pH 5 saturated CO₂ solution with 340 ppm gaseous H₂S, water + 3% NaCl, p = 1 bar, t = 20°C, ω = 1000 rpm at corrosion potential.

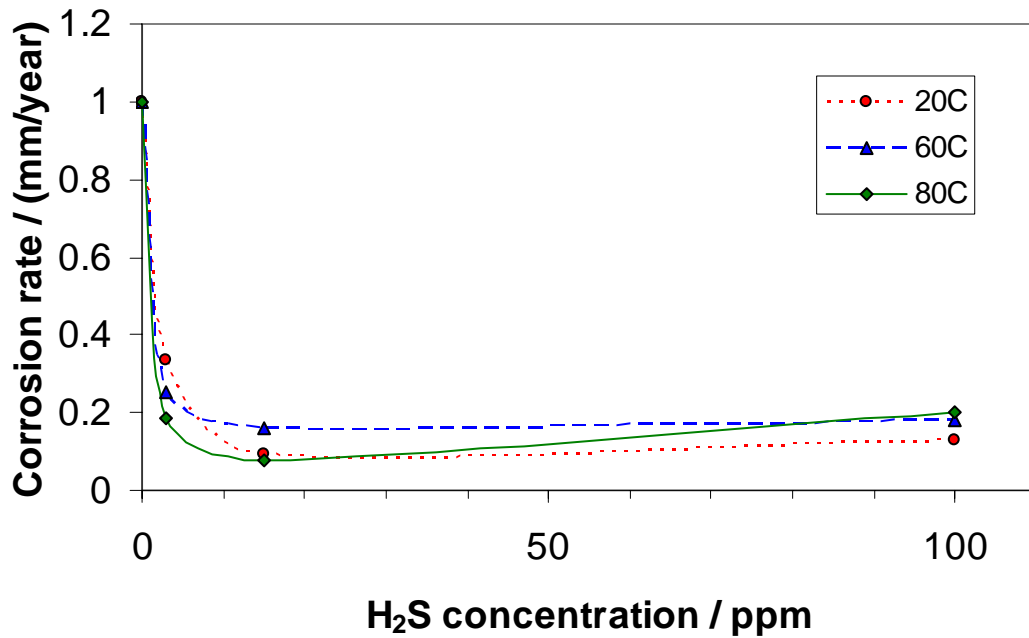


Figure 6. Normalised corrosion rate obtained under various environmental parameters in film free conditions: pH<5 p = 1-7 bar, t = 20-80°C, v=stagnant to 3 m/s.

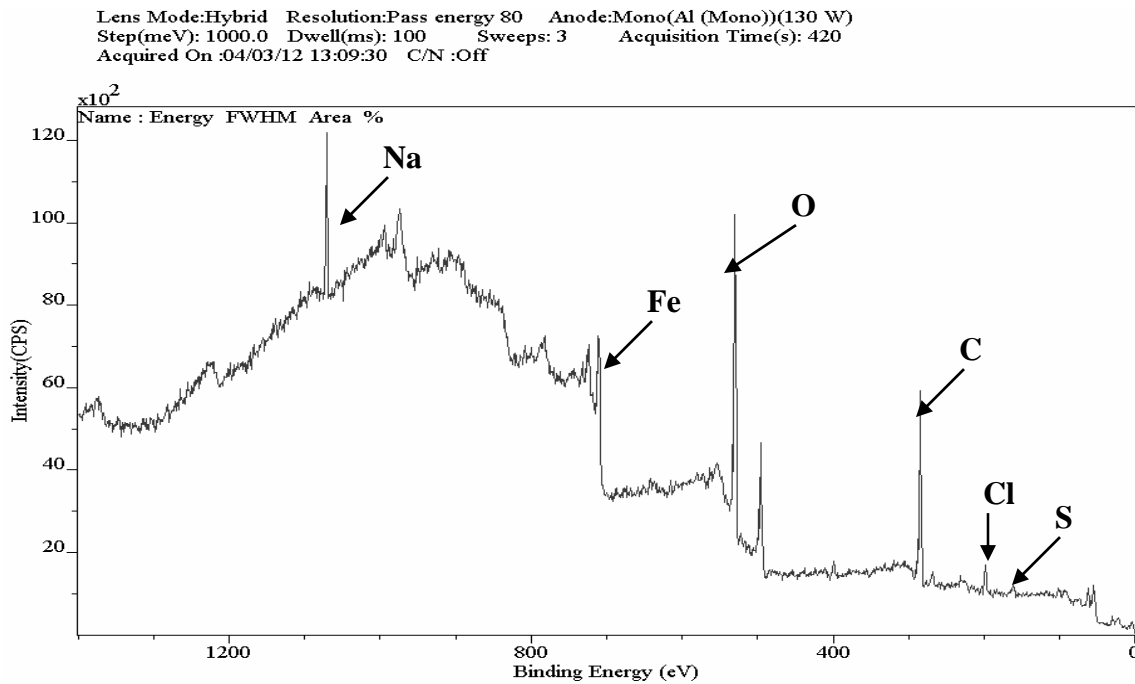


Figure 7. Survey scan on the carbon steel X65 surface after 72 hours of immersion in pH 5 saturated CO₂ solution with 340 ppm gaseous H₂S, water + 3% NaCl, p = 1 bar, t = 20°C, ω = 1000 rpm.

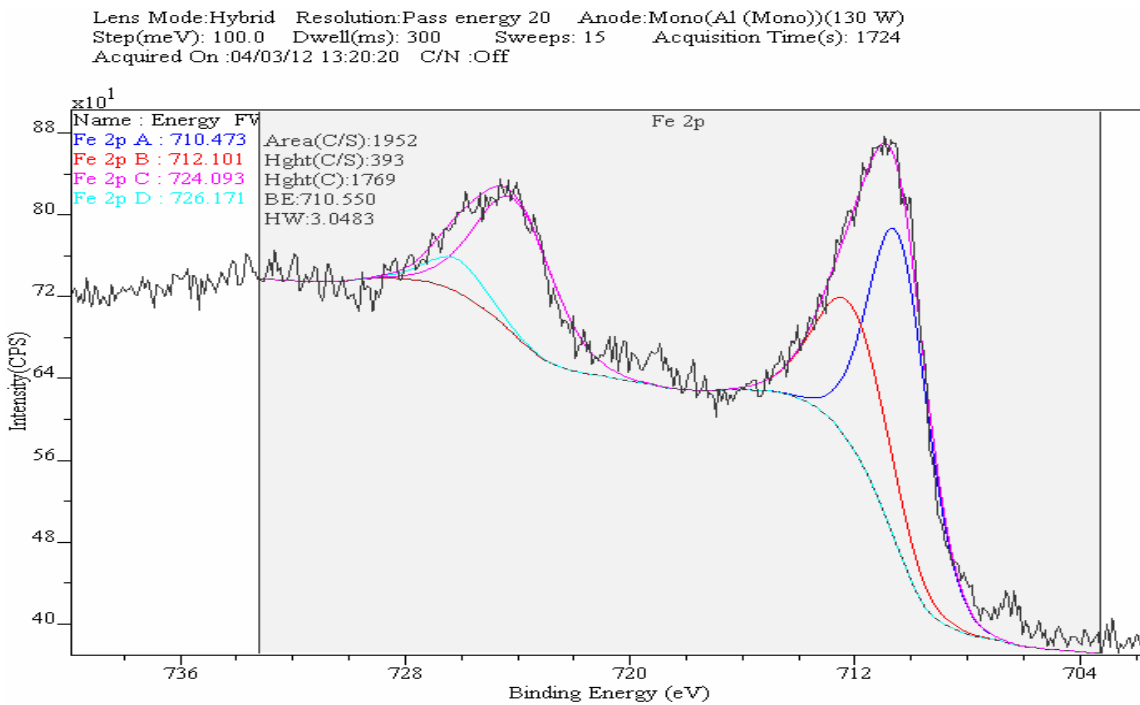


Figure 8. Narrow scans of Fe(2p_{3/2}) spectrum on the carbon steel X65 surface after 72 hours of immersion in pH 5 saturated CO₂ solution with 340 ppm gaseous H₂S, water + 3% NaCl, p = 1 bar, t = 20°C, ω = 1000 rpm , including fitted curves.

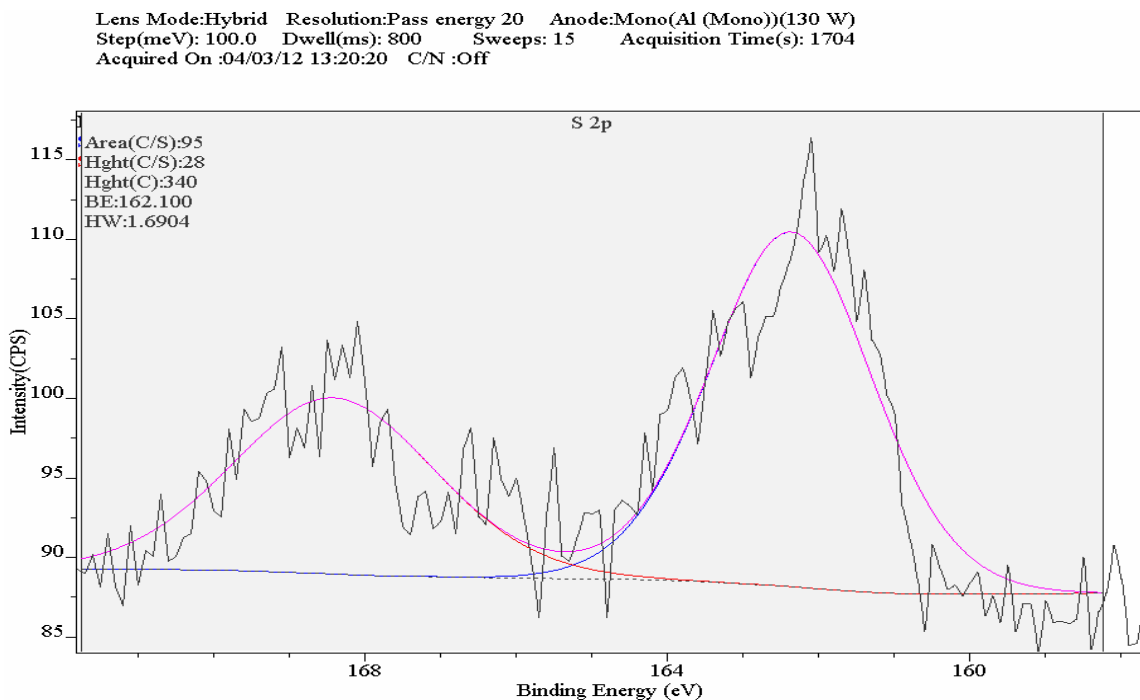


Figure 9. Narrow scans of S(2p) spectrum on the carbon steel X65 surface after 72 hours of immersion in pH 5 saturated CO₂ solution with 340 ppm gaseous H₂S, water + 3% NaCl, p = 1 bar, t = 20°C, ω = 1000 rpm, including fitted curves.

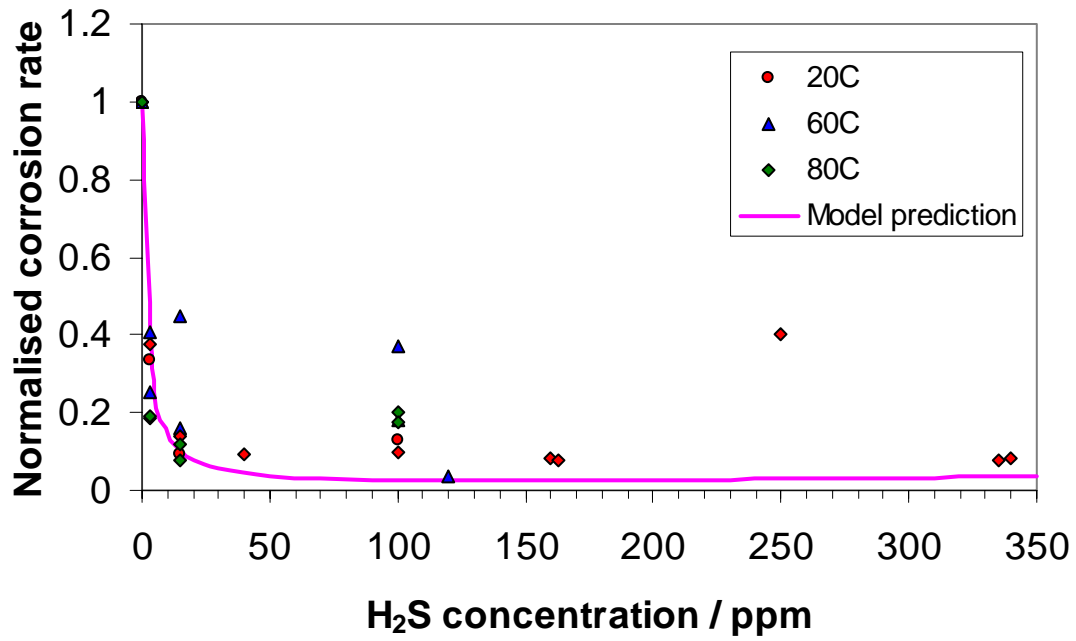


Figure 10. Comparison between model prediction and experimental data on the effect of trace amount of H₂S on CO₂ corrosion rate in the absence of iron sulfide films. .